Journal of Magnetism and Magnetic Materials 452 (2018) 297–305

Contents lists available at ScienceDirect

Journal of Magnetism and Magnetic Materials

journal homepage: www.elsevier.com/locate/jmmm

Research articles

Magnetic resonance studies of mixed chalcospinel $CuCr_2S_xSe_{4-x}$ (x = 0; 2) and $Co_xCu_{1-x}Cr_2S_4$ (x = 0.1; 0.2) nanocrystals with strong interparticle interactions

A.I. Pankrats [a,b,*], A.M. Vorotynov [a], V.I. Tugarinov [a], S.M. Zharkov [a,b], G.M. Zeer [b], K. Ramasamy [c], A. Gupta [d]

[a] Kirensky Institute of Physics, Federal Research Center KSC SB RAS, Krasnoyarsk 660036, Russia
[b] Siberian Federal University, Krasnoyarsk 660041, Russia
[c] UbiQD, LLC, 134 Eastgate Dr, Los Alamos, NM 87544, United States
[d] MINT Center, The University of Alabama, Tuscaloosa, AL 35487, United States

ARTICLE INFO

Article history:
Received 19 June 2017
Received in revised form 27 November 2017
Accepted 27 December 2017
Available online 27 December 2017

ABSTRACT

Magnetic resonance characteristics of mixed chalcospinel nanocrystals $CuCr_2S_xSe_{4-x}$ (x = 0 and 2) and $Co_xCu_{1-x}Cr_2S_4$ (x = 0.1 and 0.2) have been investigated. It has been established based on TEM, SEM and resonance data that all the samples contain both blocks with sizes from 1 to 50 m of compacted nano-sized crystallites and individual nanoparticles with sizes from 10 to 30 nm. The studies provide evidence of strong interparticle interaction in all the samples leading to high values of the blocking temperature. Magnetic dipolar field arise in the boundary regions of interacting adjacent nanocrystals below the blocking temperature. This results in inhomogeneous broadening of the magnetic resonance spectrum along with appearance of additional absorption lines. With increase in magnetic anisotropy at low temperatures, a shift of the resonance field along with line broadening are observed for all the studied compounds due to freezing of the moments in the nanoparticles, both in the individual and compacted ones. A gapped characteristic of the resonance spectrum is established below the freezing temperature T_{fr}, with the energy gap defined by the averaged magnetic anisotropy $\langle H_A \rangle$. Anionic substitution of sulfur by selenium results in a decrease in the magnetic anisotropy. In contrast, cationic substitution of copper by cobalt increases the magnetic anisotropy due to a strong contribution from the latter ion.

1. Introduction

The family of chalcogenide spinels has the general formula AB_2X_4 where X represents a chalcogen, e.g. S, Se, or Te. Among them, the chromium-based spinel family ACr_2X_4 (A = Cu, Cd, Hg, Zn, etc.) has quite broadly been investigated in bulk form, largely motivated by their unique combination of physical properties [1–5]. Room temperature ferromagnetism with the Curie temperature of 430 K makes $CuCr_2Se_4$ an interesting system for study among the chalcospinels [5]. It is metallic and exhibits a pronounced magneto-optical Kerr effect at room temperature [6]. Moreover, band structure calculations indicate that both cationic and anionic substitution of the parent compound can lead to half-metallic properties over a range of compositions [7,8].

In recent years, several other chalcospinels have renewed the interest in this class of materials because of their unique magneto-transport and magnetodielectric properties. For example, $CoCr_2S_4$ has been synthesized in the bulk and is a ferrimagnetic semiconductor with a Curie temperature around 220–240 K [9,10]. Consequently, a study of the relatively unexplored material systems $Co_{1-x}Cu_xCr_2S_4$ and $CuCr_2S_xSe_{4-x}$ is important in order to understand the competition between semiconducting and metallic characteristics and, more importantly, to ascertain if T_C shift towards room temperature is feasible in this system for practical utilization in spintronic devices. It is also significant that anionic and cationic substitutions alter the anisotropic properties of the chalcospinels. Especially large influence can be expected with Co-substitution since this ion exhibits strong magnetic anisotropy.

Nanoscale magnetic materials display unique properties such as superparamagnetism, high field irreversibility, and high saturation field due to surface anisotropy contribution [11–14]. While the magnetic properties of metallic and oxide-based nanocrystals have been studied quite extensively in recent years [15], those of chalcogenide-based materials remain largely unexplored. At nanoscale dimensions a large fraction of the atoms are present on the surface of the crystal, which can significantly alter the

* Corresponding author at: Kirensky Institute of Physics, Federal Research Center KSC SB RAS, Krasnoyarsk 660036, Russia.
E-mail address: pank@iph.krasn.ru (A.I. Pankrats).

https://doi.org/10.1016/j.jmmm.2017.12.092
0304-8853/

magnetic properties of nanostructured materials as compared to their bulk counterpart.

If the interaction between the nanoparticles is substantial, the magnetic behavior of an ensemble of particles will differ from being purely superparamagnetic. In this case, the magnetic properties of the nanoparticles are determined not only by the correlation of thermal and magnetic anisotropy energy but also by dipole-dipole interactions. Thus, if the density of the highly packed material is sufficiently high, the interparticle interactions not only modify the energy barrier arising from the anisotropy contributions of each particle but can also produce a low-temperature collective state that is completely different from the individual blocked one [16–18].

Magnetic resonance measurements provide a very sensitive probe for the study of interparticle interactions in an ensemble of nanoparticles. The magnetic resonance properties of non-interacting or weakly interacting magnetic nanoparticles are currently the subject of intense experimental and theoretical studies (see, e.g. [19–22]). Earlier we investigated the morphology-dependent magnetic resonance of $CuCr_2S_4$ nanocubes and nanoclusters [23]. Our investigation showed that at temperatures below 50 K, magnetic freezing occurs in both the nanocubes and smaller particles constituting nanocluster samples. Freezing of the magnetic moments causes a low-temperature shift of the resonance field and broadening of the resonance line. It was established that the magnetic state of the nanocubes was superparamagnetic above 50 K and up to the Curie temperature, as it should be in an ensemble of non-interacting particles. In contrast, due to interparticle interactions, the magnetic moments of the nanoclusters as a whole remained frozen above 50 K, with a blocking temperature of about 300 K, which is only slightly below the Curie temperature. Another consequence of the interparticle interaction is that in the same temperature range, additional lines appear in the resonant absorption spectra due to magnetic dipolar or exchange fields acting in the boundary regions of adjacent nanoparticles.

In this paper, we present results on magnetic resonance investigations of nanocrystals for the mixed anion and cation chalcospinels $CuCr_2S_xSe_{4-x}$ (x = 0 and 2) and $Co_xCu_{1-x}Cr_2S_4$ (x = 0.1 and 0.2). We find that the resonance properties of all the samples are characterized by specific features due to strong interparticle interaction. Scanning and transmission electron microscopy studies show a compacted state for all the samples with blocks of various sizes up to 50 μm consisting of nanosized particles. Such a morphology is responsible for the strong interparticle interaction. Comparison of the anisotropic properties shows that anion substitution of sulfur with selenium results in a decrease of the magnetic anisotropy. In contrast, cation substitution of copper ions with cobalt leads to the strong increase of the anisotropy energy.

2. Experimental

Syntheses of the mixed cation $Co_xCu_{1-x}Cr_2S_4$(x = 0.1 and 0.2) and mixed anion $CuCr_2S_{4-x}Se_x$ (x = 0 and 2) chalcospinel nanocrystals were carried out following previously reported procedures [24,25]. Briefly, $Co_xCu_{1-x}Cr_2S_4$ nanocrystals were synthesized by reacting chloride salts of copper, cobalt, and chromium with 1-dodecanethiol in octadecylamine at 360 °C. We found that use of 1-dodecanethiol as a sulfur source was necessary to form the desired phase, not only because it readily forms reactive monomer nuclei but also because it is miscible with organic capping agents and decomposes at relatively high temperatures. For the synthesis of $CuCr_2S_{4-x}Se_x$ nanocrystals, appropriate amounts of the chloride salts of Cu and Cr were mixed with octadecylamine and heated up to 360–365 °C under nitrogen. Separately, a solution with the requisite amount of diphenyldiselenide for achieving the desired mixed anion stoichiometry was dissolved in 1-dodecanthiol and then quickly introduced into the vessel containing the solution of metal salts and the was maintained at 360–365 °C for 1 h for the reaction to proceed. The mixture was then cooled down to 65–70 °C and a mixture of hexane and ethanol was added to precipitate the product. The black precipitate was isolated via centrifugation.

The morphology and size distribution of the $Co_xCu_{1-x}Cr_2S_4$ and $CuCr_2S_{4-x}Se_x$ nanocrystals were investigated using scanning and transmission electron microscopy (SEM and TEM). TEM studies were made with a JEOL JEM-2100 microscope operating at 200 kV. SEM experiments were performed with a JEOL JSM-7001F equipped with an energy dispersive X-ray spectrometer (Oxford Instruments).

The resonance spectra were collected with a Bruker spectrometer (Elexsys E580) operating at X-band frequency (ν = 9.7 GHz) in the temperature range of 110–360 K and with a wide-band magnetic resonance spectrometer with pulsed magnetic field [26]. Both the frequency-field dependences of the resonance and the temperature dependences of the resonance fields and linewidths were measured.

3. Results

Temperature evolutions of the X-band spectra of $CuCr_2S_xSe_{4-x}$ (x = 0 and 2) nanocrystals are shown in Fig. 1. With lowering the temperature two resonance peaks can be seen (the weak low-field peak is marked by an arrow) at temperatures below 300 K for the $CuCr_2S_2Se_2$ spectra, while a single line is observed for $CuCr_2Se_4$ at all the temperatures. The experimental resonance spectra of $CuCr_2S_2Se_2$ were approximated by the sum of two single resonance lines, the typical example of such a deconvolution for

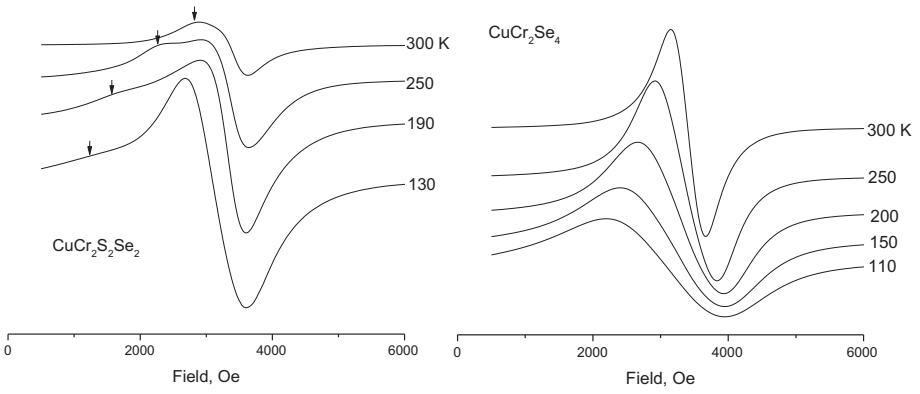

Fig. 1. Temperature evolution of the X-band spectra for the $CuCr_2S_2Se_2$ (a) and $CuCr_2Se_4$ (b) nanocrystals.

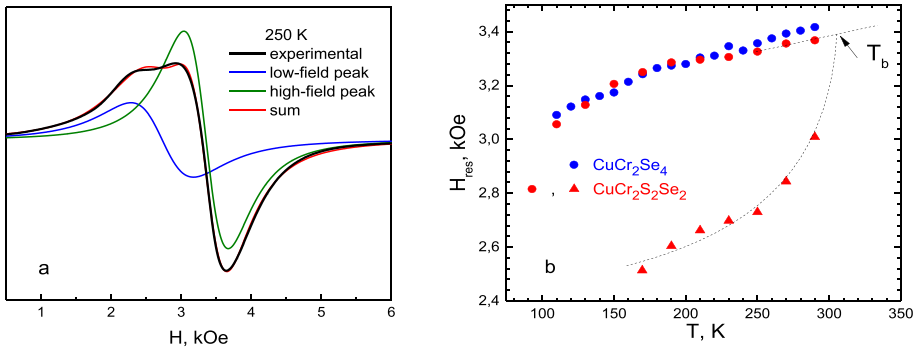

Fig. 2. a – approximation of $CuCr_2S_2Se_2$ spectra at T = 250 K by the sum of two single resonance lines, b – temperature dependences of the resonance fields in $CuCr_2Se_4$ and for two resonance peaks in $CuCr_2S_2Se_2$.

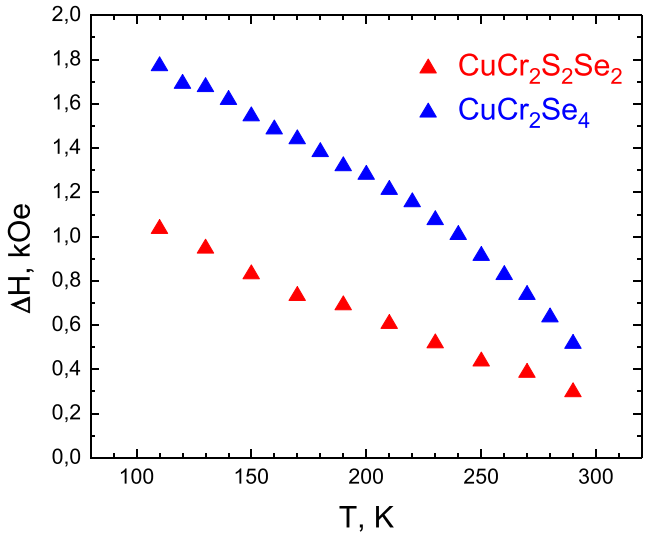

Fig. 3. Temperature dependences of the linewidth in $CuCr_2Se_4$ nanocrystals and for the high-field peak in $CuCr_2S_2Se_2$ nanocrystals.

$CuCr_2S_2Se_2$ spectra at T = 250 K is depicted in Fig. 2a. The temperature dependences of the resonance fields in $CuCr_2Se_4$ and for two resonance peaks in $CuCr_2S_2Se_2$ are shown in Fig. 2b.

Fig. 3 presents the temperature dependences of the linewidths in $CuCr_2S_xSe_{4-x}$ (x = 0 and 2). The linewidth in $CuCr_2Se_4$ is almost twice the width of the main high-field peak in $CuCr_2S_2Se_2$. This may be a possible reason why splitting of the resonance line in the $CuCr_2Se_4$ sample is not visible with lowering the temperature.

The resonance properties at low temperatures have been studied using the wide-band resonance spectrometer, with typical spectra for $CuCr_2Se_4$ and $CuCr_2S_2Se_2$ presented in Fig. 4a and b for two different temperatures. The frequency-field dependencies of FMR in $CuCr_2S_2Se_2$ and $CuCr_2Se_4$ measured at 4.2 and 180 K are shown in Fig. 4b. For both samples, the dependencies are linear at both temperatures and gapless at T = 180 K. The temperature dependences of the resonance field and linewidth for $CuCr_2S_2Se_2$ are shown in Fig. 5. Both a sharp decrease in the resonance field and broadening of the resonance line are observed below a certain characteristic temperature of freezing $T_{fr} \approx 70$ K, as in the $CuCr_2S_4$ nanoparticles [23]. A gapped character of the magnetic resonance is established for both samples at T = 4.2 K, with the gap defined by the mean value of the anisotropy field $\langle H_A \rangle$, similar to that observed for $CuCr_2S_4$ nanoparticles [23]:

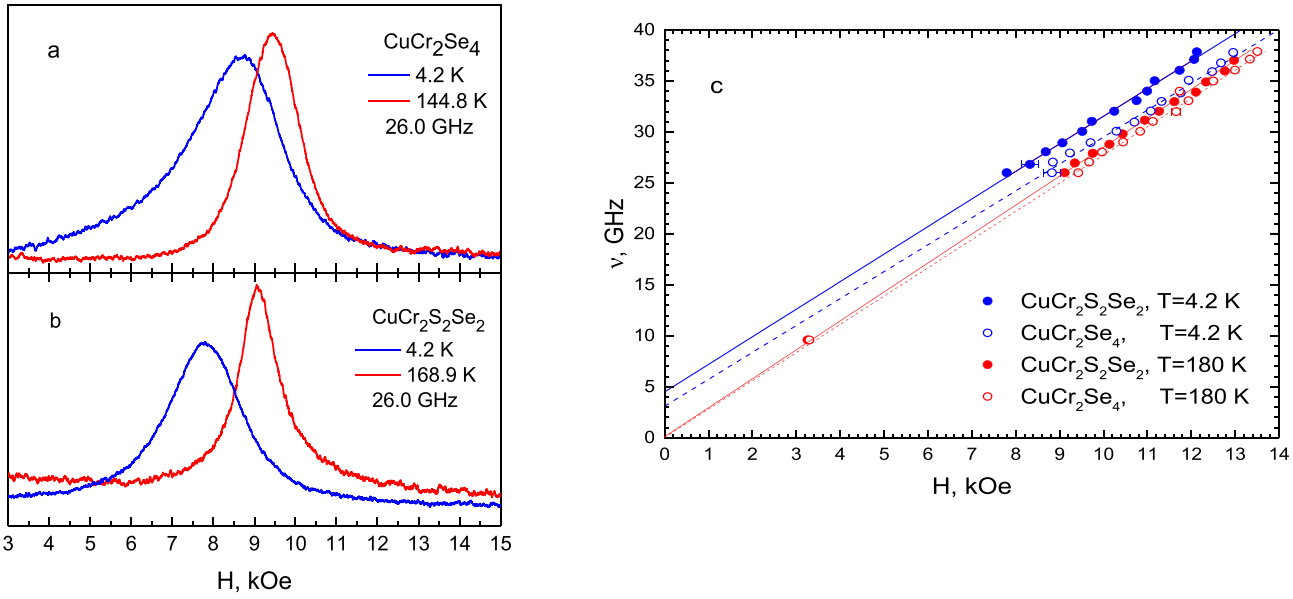

Fig. 4. Resonance spectra of $CuCr_2Se_4$ (a) and $CuCr_2S_2Se_2$ (b), c – frequency-field dependences of FMR in $CuCr_2S_2Se_2$ (closed circles) and $CuCr_2Se_4$ (open circles), T = 4.2 K (blue), T = 180 K (red). (For interpretation of the references to colour in this figure legend, the reader is referred to the web version of this article.)

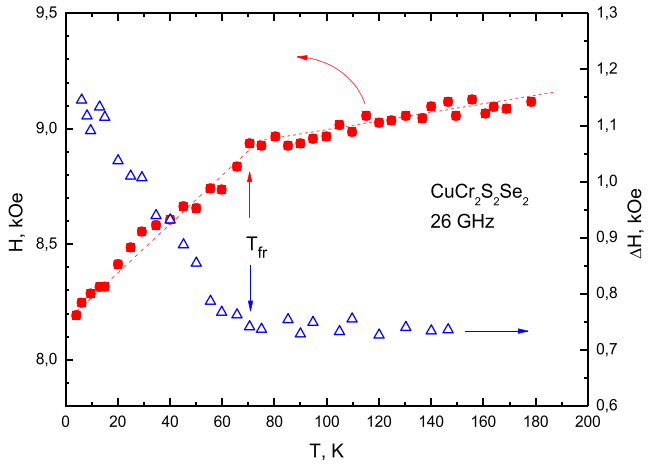

Fig. 5. Temperature dependences of the resonance field and the linewidth in $CuCr_2S_2Se_2$ nanoparticles at frequency ν = 26.0 GHz.

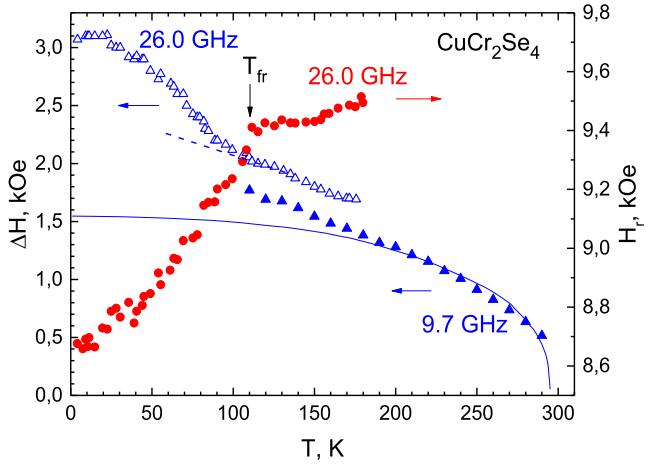

Fig. 6. Temperature dependences of the resonance field (red circles) and the linewidth (open blue triangles) for $CuCr_2Se_4$ nanoparticles at the frequency ν = 26.0 GHz and in the X-band (closed blue triangles). The solid line shows the normalized temperature dependence of the saturation magnetization of bulk $CuCr_2Se_4$ from [27]. (For interpretation of the references to colour in this figure legend, the reader is referred to the web version of this article.)

$$\frac{\nu}{\gamma} = H + \langle H_A \rangle. \quad (1)$$

In accordance with this equation, the linear fit of the experimental frequency-field dependences (blue lines in Fig. 4c) leads to the following values of the parameters at T = 4.2 K: the energy gaps $\nu_c = \gamma\langle H_A \rangle$ are (4.5 ± 0.6) kOe and (3.1 ± 0.8) kOe with the gyromagnetic ratios (2.70 ± 0.06) GHz/kOe and (2.65 ± 0.08) GHz/kOe for $CuCr_2S_2Se_2$ and $CuCr_2Se_4$, respectively. With decreasing temperature, broadening of the resonance line commences below T_{fr} due to random variation of the directions of easy magnetization in the ensemble of nanoparticles. In contrast with the X-band data, the linewidth remains essentially constant above the critical temperature up to 150 K.

A similar temperature dependence of the resonance field is observed for the $CuCr_2Se_4$ nanoparticles (see Fig. 6). But in this case the freezing temperature $T_{fr} \approx 110$ K is significantly higher than that for $CuCr_2S_2Se_2$. Fig. 6 also shows the temperature dependence of the high-frequency linewidth which too has a well-pronounced kink at the temperature T_{fr}. The high-frequency linewidth is slightly higher than the X-band data depicted here as well. The X-band linewidth tends to zero when approaching the Curie temperature. This dependence is qualitatively described at high temperatures by the normalized temperature dependence of the saturation magnetization of bulk $CuCr_2Se_4$ [27].

Similar behavior of the magnetic resonance properties is observed in cation substituted $Co_xCu_{1-x}Cr_2S_4$ for x = 0.1. Fig. 7a presents the temperature dependences of the resonance fields for two resonance peaks observed in $Co_{0.1}Cu_{0.9}Cr_2S_4$ at X-band. At high temperatures, a single line is observed with the parameters: ΔH ≅ 400 Oe, H_{res} ≅ 3390 Oe. At the blocking temperature T_b ≅ 235 K this splits into two lines, with the blocking temperature being very close to the Curie point T_C = 250 K which is slightly lower than the value 265 K found in [24]. This splitting monotonously increases with lowering the temperature, reaching the maximal value at T ≅ 150 K and remains practically unchanged with further lowering of the temperature.

Fig. 7b presents the temperature dependences of the linewidths of two resonance lines observed in $Co_{0.1}Cu_{0.9}Cr_2S_4$ at X-band. The high field (open circles in Figs. 7, 8) resonance linewidth monotonously increases with lowering the temperature with a small disruption at T ≅ 236 K, where line splitting is observed. The width of the line appearing at T ≅ 236 K (closed circles in Figs. 7, 8) rises significantly with further decrease in the temperature, reaching a maximal value ΔH ≅ 2500 Oe at T ≅ 165 K and then drops down at lower temperatures.

In case of the $Co_xCu_{1-x}Cr_2S_4$ (x = 0.2) sample, the observed resonance spectrum differs from that of the sample with x = 0.1. At high temperatures, the initial spectrum consists of two lines (see Fig. 8). Additionally, a third line appears in the spectrum below T_b ≅ 220 K. Its resonance field decreases rapidly with lowering the temperature (Fig. 8a) and reaches a plateau at T ≈ 200 K. The width of this line smoothly decreases with decreasing temperature with also an anomaly at T ≅ 220 K (Fig. 8b). One of the initial main lines exhibits a noticeable anomaly at the blocking temperature, both in the resonance field and the linewidth. The temperature

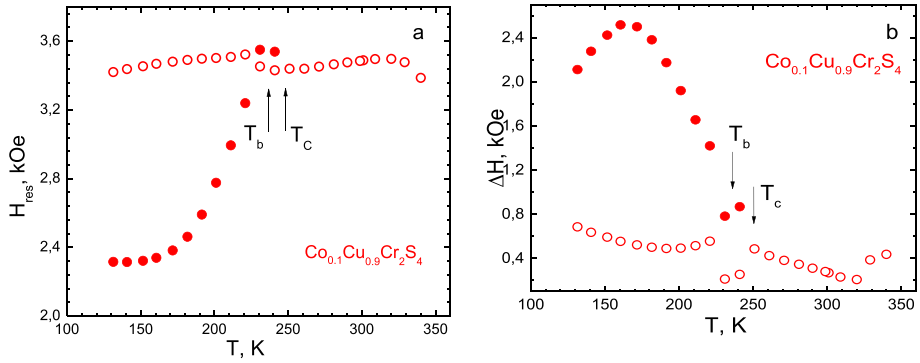

Fig. 7. Temperature dependences of the resonance fields (a) and the linewidths (b) for $Co_{0.1}Cu_{0.9}Cr_2S_4$ measured at X-band.

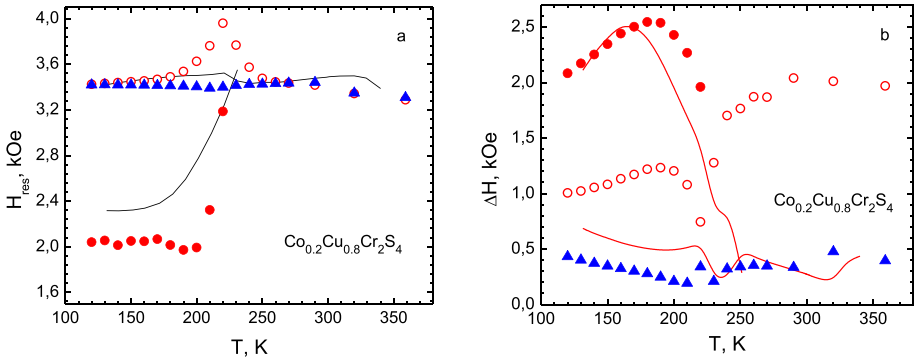

Fig. 8. Temperature dependences of the resonance fields (a) and the linewidths (b) for $Co_{0.2}Cu_{0.8}Cr_2S_4$. The solid lines present the data for the $Co_{0.1}Cu_{0.9}Cr_2S_4$ sample for comparison.

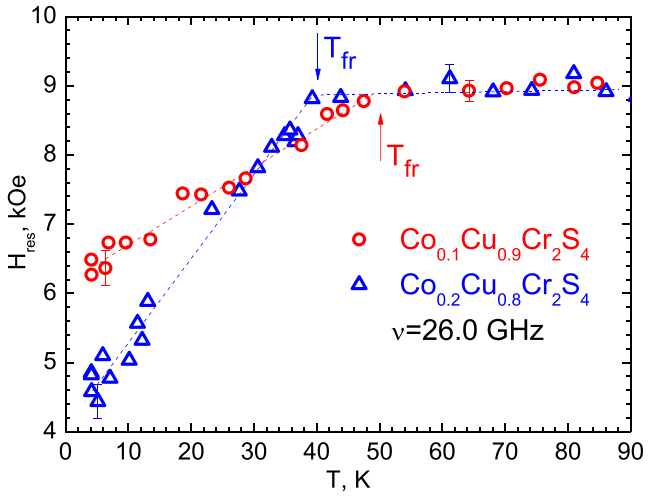

Fig. 9. Temperature dependences of the resonance fields in nanoparticles $Co_{0.1}Cu_{0.9}Cr_2S_4$ and $Co_{0.2}Cu_{0.8}Cr_2S_4$.

dependences of the linewidths for the additional lines are similar for samples with x = 0.1 and 0.2.

We believe that the appearance of the double line in the resonance spectrum of $Co_{0.2}Cu_{0.8}Cr_2S_4$ at temperatures above T_C, in contrast to the single resonance line of $Co_{0.1}Cu_{0.9}Cr_2S_4$, may be due to some structural defects (for example, twin boundary defects and inhomogeneous strain) in the sample. The presence of such defects in $Co_xCu_{1-x}Cr_2S_4$ at a small x-concentration is clearly observed in [24].

The temperature dependences of the resonance fields measured at the frequency ν = 26.0 GHz are shown in Fig. 9. In both compounds, the resonance fields are independent of temperature above the appropriate freezing temperatures T_{fr} (about 40 K and 50 K for $Co_{0.1}Cu_{0.9}Cr_2S_4$ and $Co_{0.2}Cu_{0.8}Cr_2S_4$, respectively). The values of the resonance frequencies in this temperature range correspond to Eq. (1) with $\langle H_A \rangle$ tending to zero. Below T_{fr}, the resonance fields decrease rapidly indicating the appearance of the energy gap $\nu_c = \gamma\langle H_A \rangle$ in the spectrum. To determine the mean values of the anisotropy field $\langle H_A \rangle$, we used the gyromagnetic ratios γ found at room temperature from the X-band investigations: (2.77 ± 0.03) GHz/kOe and (2.79 ± 0.03) GHz/kOe for x = 0.1 and 0.2 samples, respectively. The value of $\langle H_A \rangle \approx 4.4$ kOe in $Co_{0.2}Cu_{0.8}Cr_2S_4$ at T = 4.2 K, with this value being the highest among all the nanoparticles studied here. Unfortunately, due to the small amounts of the samples and the lower sensitivity of the wide-band spectrometer, we could not measure the temperature dependences of the linewidth for these two samples with the required accuracy. But qualitatively, the linewidths increase rapidly below the freezing temperatures in both compounds as in $CuCr_2S_xSe_{4-x}$ nanoparticles.

4. Discussion

For explanation of the magnetic resonance data in the examined nanoparticles, it is useful to compare them with previous magnetic resonance results [23] obtained for two types of $CuCr_2S_4$ nanoparticles, prepared using slightly different techniques.

It has been shown in [23] that when using oleylamine (OLA) as a solvent, nanoclusters with sizes from 80 to 140 nm composed of smaller particles are formed, as determined by TEM and HRTEM examinations. Due to strong interparticle interactions in a cluster, the magnetic moment of the whole nanocluster is blocked at temperatures slightly lower than the Curie point. Below the blocking temperature, an additional line appears in the resonance spectrum due to interparticle interaction as well. The magnetic anisotropy energy of the individual nanoparticles composing the cluster increases with decreasing temperature, which leads to freezing of the magnetic moment of the individual nanoparticles at temperatures below $T_{fr} \approx 60$ K. This process is accompanied by additional anomalies of the temperature dependences of FC and ZFC magnetizations at this temperature T_{fr}, the appearance of an energy gap in the spectrum of magnetic resonance and line broadening below ~60 K. This broadening is caused by the random distribution of both directions of the easy magnetization in the individual particles composing the cluster and the values of the effective fields induced by the interparticle interactions.

In contrast, nanoparticles prepared using octadecylamine (ODA) as a solvent consist of separate cube-shaped nanocrystals with negligible interparticle interaction [23]. With lowering the temperature, a single resonance line with close to a Lorentzian shape is observed for the nanocubes at all temperatures. The temperature dependences of the FC and ZFC magnetizations show a single anomaly at T ≈ 50 K, corresponding to blocking of the magnetic moments of the nanocubes. In the blocked state, an energy gap in the spectrum of magnetic resonance and line broadening appears as well, but the linewidth observed in the nanocubes is remarkably lower than that in the nanoclusters.

Considering these peculiarities, we can conclude that all the samples examined in this work are characterized by strong interparticle interactions. The primary type of the interaction is dipole-dipole type, but the exchange interaction contribution between the particles can also be noticeable for a high degree of compactness. The important signature of such an interaction is the appearance of an additional line in the magnetic resonance spectrum. Only $CuCr_2Se_4$ did not reveal resonance splitting at all temperatures. However, the resonance linewidth in this sample

is about two times larger than that in $CuCr_2S_2Se_2$. Such a strong broadening can be caused just by the interparticle interactions, the values of which have a large spread due to the random distribution of the particle size or composition. In this case, the resonance absorption line is the envelope of many individual lines. The temperature dependence of the linewidth of the resonance spectrum, in this case, should be determined by the temperature dependence of magnetization. In Fig. 6, the solid line shows the normalized temperature dependence of magnetization, taken from [27] for the bulk $CuCr_2Se_4$; indeed, this dependence describes qualitatively the behavior of the linewidth at high temperatures. As mentioned above, the freezing of the magnetic moments in the individual nanoparticles causes a shift in the resonance line due to the gap in the spectrum and additional line broadening. The most significant changes in the resonance field and linewidth are observed below a characteristic temperature of the low temperature freezing $T_{fr} \approx 110$ K, but due to the dispersion of the particle sizes the contribution of these processes become noticeable even at temperatures above T_{fr} up to ~180 K.

Note that, as in $CuCr_2S_4$ nanoclusters [23], all samples studied have high blocking temperatures T_B close to the respective Curie points. For non-interacting nanoparticles of volume $V = d^3$, anisotropy constant K_{eff} and characteristic measurement time τ_m, the blocking temperature T_B is determined by the well-known relation (see e.g.: [28]):

$$T_B = \frac{K_{eff} V}{\ln(\tau_m/\tau_0) k_B} \tag{2}$$

where k_B is the Boltzmann's constant and the typical values of the characteristic flip time τ_0 depend on the parameters such as temperature, magnetization, gyromagnetic ratio, anisotropy constant, etc., and are in the interval 10^{-13}–10^{-10} s.

Using Eq. (2) with $K_{eff} = 0.9 \cdot 10^5$ erg/cm^3 at T = 295 K determined for the bulk compound $CuCr_2Se_4$ [27] and $T_B = 385$ K determined for the nanoparticles [25], the particle size is estimated as $d \approx 26$ nm which is more than twice larger than the experimental value $\langle d \rangle = 12$ nm obtained by TEM [25].

On the other hand, considering the real temperature dependence of the anisotropy constant [27], the estimation of the blocking temperature for the non-interacting $CuCr_2Se_4$ particles of the size $\langle d \rangle = 12$ nm gives $T_B = 120$ K, which is lower than the value of $T_B = 385$ K obtained in [25]. Apparently, the same situation with the description of the blocking temperatures is implemented in other studied samples in which the sizes of the nanoparticles are similar to that of $CuCr_2Se_4$ and the blocking temperatures are also high and close to the corresponding Curie points. Thus, we can say that the model of non-interacting nanoparticles gives incorrect evaluation of the blocking temperatures in the studied samples.

In accordance with the approach of the random anisotropy model (RAM) suggested in [29] for interacting nanoparticles, such a large discrepancy can be explained by the fact that in the case of interacting particles, the blocking temperature is determined by the clusters whose effective volumes are defined by the correlation length L_H depending on the magnetic field H:

$$L_H = d + \sqrt{\frac{2A_{eff}}{M_S H + C}}, \tag{3}$$

here A_{eff} represents the interparticle interaction strength, M_S is the saturation magnetization and the constant C accounts for the interaction strength variation with the particle filling factor and plays an important role only for field values close to zero. In this case, the anisotropy constant also changes as

$$K_{eff} \rightarrow K^*_{eff} \equiv \frac{K_{eff}}{\sqrt{N}} = \frac{K_{eff}}{\sqrt{1 + x\left(L_H^3 - d^3\right)/d^3}}, \tag{4}$$

where N is the number of the correlated particles in the cluster and x is the volume concentration of the substance (filling factor).

The field dependence of the blocking temperature for the non-interacting particles is described as [30]:

$$T_B = \frac{K_{eff} V}{\ln(\tau_m/\tau_0) k_B} \left(1 - \frac{M_S H}{2K_{eff}}\right)^{3/2}. \tag{5}$$

In the frame of RAM, the interparticle interaction transforms this Equation into [29]:

$$T_B(H) = \frac{K^*_{eff}\left[d^3 + x(L_H^3 - d^3)\right]}{k_B \ln(\tau_m/\tau_0)} \left(1 - \frac{M_S H}{2K^*_{eff}}\right)^{3/2}, \tag{6}$$

where K^*_{eff} is defined in (4).

It is interesting to analyze the experimental magnetic field dependences of the blocking temperatures for the $CuCr_2S_2Se_2$ and $CuCr_2Se_4$ compounds from magnetic measurements [25], which are presented in Fig. 10. In both compounds, the blocking temperature decreases with increasing magnetic field. We used the expressions (5) and (6) to fit the experimental data of Fig. 10. Both fits are carried out using $M_S = 348$ G (the bulk value at T = 0 K [27]) and A_{eff}, K_{eff}, d and C as free parameters. The dotted and solid lines in Fig. 10 present the best fits to Eqs. (5) and (6). It is obvious, that Eq. (6) for the interacting particles better describes the experimental data for both compounds. The parameters of fitting providing the best description of the blocking temperatures are summarized in Table 1.

The particle sizes determined from these fits are close to the average sizes determined by TEM [25]. It is interesting, that the correlation length, defining the effective volume of the clusters in $CuCr_2Se_4$, $L_0 = 26.3$ nm (as $H \rightarrow 0$), coincides well with the particle sizes $d = 26$ nm which was estimated above from the blocking temperature for this nanoparticles using Eq. (2). The comparison shows that the correlation lengths L_0 defining the sizes of the clusters in both compounds are significantly larger than the real sizes of the nanoparticles. The anisotropy constant K_{eff} of $CuCr_2Se_4$ is close to the experimental bulk value and approximately exceeds two times the constant in $CuCr_2S_2Se_2$; such a relation between the constants in these compounds is valid for both interactive and non-interactive descriptions. Close values of the interparticle interaction strength A_{eff} and the ratio L_0/d were also obtained for interacting nanoparticles of $Co_x(SiO_2)_{1-x}$ [29] and magnetite [31].

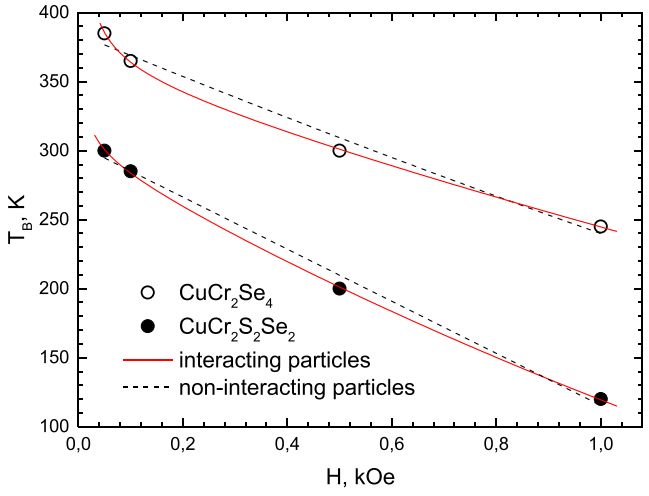

Fig. 10. Magnetic field dependences of the blocking temperatures of $CuCr_2S_2Se_2$ and $CuCr_2Se_4$ nanoparticles from magnetic measurements [12].

Table 1
Best fit parameters of the effective anisotropy constant K_{eff}, the particles sizes d (in both interactive and non-interactive descriptions), the interparticle interaction strength A_{eff} and the correlation length L_0.

Compound	Non-interacting particles		Interacting particles			
	K_{eff}, 10^5 erg/cm^3	d, nm	K_{eff}, 10^5 erg/cm^3	d, nm	L_0, nm	A_{eff}, 10^{-9} erg/cm
$CuCr_2S_2Se_2$	2.8 ± 0.1	15.7 ± 0.3	4.0 ± 0.2	13.6 ± 0.4	18.4 ± 0.5	2.6 ± 0.3
$CuCr_2Se_4$	4.7 ± 0.2	14.3 ± 0.5	8.1 ± 0.3	11.6 ± 0.5	26.3 ± 0.6	1.6 ± 0.5

A question arises why the interparticle interaction is almost negligible in the nanocubes $CuCr_2S_4$ [23] but is present in the nanoparticles of $CuCr_2S_2Se_2$ and $CuCr_2Se_4$ prepared using a similar technique.

The SEM investigations show that the $Co_xCu_{1-x}Cr_2S_4$ and $CuCr_2S_{4-x}Se_x$ samples consist of blocks with sizes varying from 1 to 50 μm and nanoparticles (see, for example, Fig. 11a, c), whereas TEM shows only 10–30 nm size particles (see, for example, Fig. 11b, d). So, it can be supposed that the blocks are formed from the same nanoparticles. This idea is supported by the observation of pronounced temperature anomalies (see, the freezing temperatures T_{fr} in Figs. 5, 6 and 9) in the temperature dependences of the resonance fields. Based on the analysis of the SEM data one can conclude that the main contribution to the resonance absorption is due to the nanoparticles forming the blocks. The formation of the compacted blocks may be a result of drying the solution suspension.

The low-temperature anomalies of the resonance properties below the specific freezing temperatures, which are suggested by the sharp decrease of the resonance field and the broadening of the absorption line, are observed in all the samples studied here and have a common origin. As in $CuCr_2S_4$ nanoparticles studied earlier [23], the freezing of the magnetic moments in the individual nanoparticles causes a shift of the resonance line due to the appearance of a gap in the spectrum and an additional line broadening. Strictly speaking, the magnetic state in all the mentioned samples above the low-temperature anomalies (40–50 K in the samples $Co_xCu_{1-x}Cr_2S_4$ and 70–110 K in the samples $CuCr_2S_{4-x}Se_x$) is frozen within a cluster size defined by the correlation length (3). In this case, the resonance properties in such a state should also obey Eq. (1). However, due to the random orientations of the easy axis of magnetization of the nanoparticles in a cluster, the effective magnetic anisotropy for this cluster is weakened in accordance with Eq. (4). The weakening of the anisotropy increases when a greater number of nanoparticles is included into the volume of the cluster. Accordingly, above the low-temperature anomalies, very weak temperature dependences of the resonance field are observed in the nanoparticles of $CuCr_2S_2Se_2$ and $CuCr_2Se_4$ (see

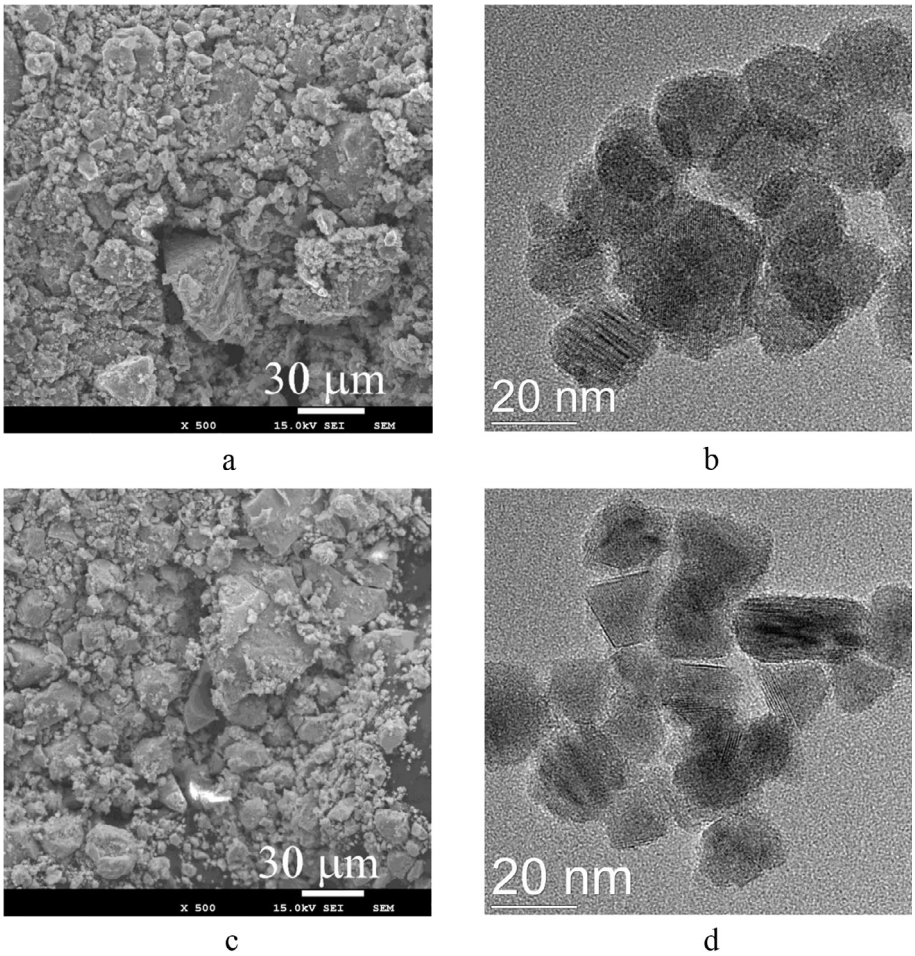

Fig. 11. SEM (a, c) and TEM (b, d) images of $Co_{0.1}Cu_{0.9}Cr_2S_4$ and $CuCr_2S_2Se_2$, respectively.

Table 2
Temperatures of freezing T_{fr} and the average magnetic anisotropy field of the nanoparticles measured at T = 4.2 K.

Compounds	$CuCr_2Se_4$	$CuCr_2S_2Se_2$	$CuCr_2S_4$ [23]	$Co_{0.1}Cu_{0.9}Cr_2S_4$	$Co_{0.2}Cu_{0.8}Cr_2S_4$
T_{fr}, K	110	70	60	38	48 (25)*
$<H_A>$, kOe	1.2 ± 0.3	1.7 ± 0.2	2.5	2.5 ± 0.2	4.4 ± 0.3

* The freezing temperature determined by MPMS magnetic measurements in [24].

Figs. 2, 5 and 6) and the resonance fields are practically independent of the temperature in $Co_xCu_{1-x}Cr_2S_4$ (Figs. 7a, 8a and 9). At low temperatures, when the magnetic anisotropy becomes sufficiently strong, the freezing of the magnetic moments in each of the nanoparticles constituting a cluster occurs, leading to the shift of the resonance field and widening of the resonance lines. The shift is caused by the appearance of the average magnetic anisotropy fields (1) whose magnitudes measured at T = 4.2 K for all the studied nanoparticles are shown in Table 2.

If we start from a reasonable assumption that there is a correlation between the anisotropy constant and its averaged value, the comparison shows that the cationic substitution of copper ions with cobalt leads to a strong increase of the anisotropy energy. Such a result is expected as the cobalt ion is characterized by a strong magnetic anisotropy. In contrast, the anionic substitution of sulfur with selenium should result in a decrease of the magnetic anisotropy. Such a conclusion contradicts the results of Table 1 where the anisotropy constant for $CuCr_2Se_4$ is twice that for $CuCr_2S_2Se_2$. Such a contradiction indicates that the anisotropy constants estimated for the interacting particles from the blocking temperatures should be considered with caution.

The analysis suggests that the $Co_xCu_{1-x}Cr_2S_4$ and $CuCr_2S_xSe_{4-x}$ nanoparticles synthesized and examined in [24,25] are also characterized by strong interparticle interactions. These interactions are responsible for the high values of the blocking temperatures in the nanoparticles, found both in our resonance studies and in the magnetic measurements [24,25]. We also assume that because of these interactions, the volumes of the clusters whose sizes are defined by the correlation lengths are so large that the blocking of the magnetic moments in the clusters occurs at temperatures very close to the Curie point. In other words, the freezing of the moments within the correlation volume occurs as soon as the magnetization is sufficiently large at temperatures below T_C.

Note also that the magnetic measurements established that all the nanoparticle samples studied in [24,25] show two anomalies in the temperature dependences of the magnetization. The high-temperature anomaly is responsible for the above-mentioned freezing of the magnetic moment in the volume of the clusters and the low-temperature one is caused by the freezing of the moment in each of the nanoparticles, in both individual and compacted particles.

It is also important that judging from the temperature dependences of the magnetization [24,25] and the frequency-field dependences of the resonance measured at T = 4.2 K, the low-temperature anomaly is caused by the freezing process occurring throughout the volume of the samples including the compacted blocks. This indicates that the compacted blocks also consist of the nanoparticles with the sizes close to those of the individual particles.

Thus, the predominantly compacted state of the nanoparticles studied in this paper causes a strong interaction between the particles. In turn, this leads to the fact that the values of the blocking temperatures of the magnetic moments are extremely high and close to the corresponding values of the Curie temperatures. As a result, high values of the magnetization are possible in the nanocrystalline spinels at room temperatures, exceeding the magnetization of the superparamagnetic ensembles of non-interacting or weakly interacting particles. Such a property can be extremely useful for practical applications of nanoscale magnetic materials.

5. Conclusion

Mixed composition nanocrystals of $Co_xCu_{1-x}Cr_2S_4$ and $CuCr_2S_x$-Se_{4-x}were synthesized by a facile colloidal method. Structural and magnetic resonance investigations were carried out in the anionic and cationic substituted chalcogenide spinel nanocrystals Co_x-$Cu_{1-x}Cr_2S_4$ (x = 0.1, 0.2) and $CuCr_2S_xSe_{4-x}$ (x = 0, 2). It was established based on TEM and SEM studies that all the samples contained both blocks with sizes from 1 to 50 m of compacted nanosized crystallites and individual nanoparticles with the sizes from 10 to 30 nm.

Due to the compacted state of the samples, strong interparticle interaction plays an important role in dictating the magnetic properties of the samples studied. There are two main consequences of interparticle interaction: (i) high values of the blocking temperature caused by the freezing of the magnetic moments in the nanoclusters whose effective volumes are determined by the correlation length; (ii) inhomogeneous broadening of the magnetic resonance spectrum and the appearance of additional absorption lines in the spectrum below the blocking temperature caused by the effective magnetic field acting in the boundary regions of the interacting adjacent constituent nanocrystals.

With increase of the magnetic anisotropy at low temperatures, a shift of the resonance fields and line broadening occur in all the studied compounds due to the freezing of the moments in the nanoparticles, both in the individual and compacted ones. The gapped character of the resonance spectrum is established below the freezing temperature T_{fr}, with the energy gap defined by the averaged magnetic anisotropy $<H_A>$.

The anionic substitution of sulfur by selenium results in a decrease of the magnetic anisotropy. In contrast, cationic substitution of the copper ions by cobalt increases the magnetic anisotropy due to strong contribution of the cobalt ions.

Acknowledgments

The authors thank D.A. Balaev for fruitful and useful discussions. The work at the University of Alabama was supported by the National Science Foundation, United States under Grant No. CHE-1508259.

References

[1] F.K. Lotgering, Solid State Commun. 2 (1964) 55.
[2] F.K. Lotgering, Proceedings of the International Conference on Magnetism, Nottingham (1964) 533.
[3] P.K. Baltzer, H.W. Lehmann, M. Robbins, Phys. Rev. Lett. 15 (1965) 493.
[4] J.B. Goodenough, J. Phys. Chem. Solids 30 (1969) 261.
[5] K.G. Nikiforov, Prog. Cryst. Growth Charact. Mater. 39 (1999) 1.
[6] H. Brandle, J. Schoenes, P. Wachter, F. Hulliger, Appl. Phys. Lett. 56 (1990) 2602.
[7] Y.-H.A. Wang, A. Gupta, M. Chshiev, W.H. Butler, Appl. Phys. Lett. 92 (2008) 062507.
[8] Y.-H.A. Wang, A. Gupta, M. Chshiev, W.H. Butler, Appl. Phys. Lett. 94 (2009) 062515.
[9] K. Ohgushi, Y. Okimoto, T. Ogasawara, S. Miyasaka, Y.M. Tokura, J. Phys. Soc. Jpn. 77 (2008) 034713.
[10] V. Sagredo, M.C. Moron, G.E. Delgado, Phys. B 384 (2006) 82.

[11] X. Batlle, A. Labarta, J. Phys. D: Appl. Phys. 35 (2002) R15.
[12] J. Frenkel, J. Dorfman, Nature 126 (1930) 274.
[13] C.P. Bean, J.D. Livingston, J. Appl. Phys. 30 (1959) 1205.
[14] A.J. Zarur, J.Y. Ying, Nature 403 (2000) 65.
[15] D. Fiorani, Surface Effects in Magnetic Nanoparticles, Springer, Berlin, 2005.
[16] S. Bedanta, W. Kleemann, J. Phys. D: Appl. Phys. 42 (2009) 013001.
[17] W. Kleemann, O. Petracic, C. Binek, G.N. Kakazei, Y.G. Pogorelov, J.B. Sousa, S. Cardoso, P.P. Freitas, Phys. Rev. B 63 (2001) 134423.
[18] O. Petracic, X. Chen, S. Bedanta, W. Kleemann, S. Sahoo, S. Cardoso, P.P. Freitas, J. Magn. Magn. Mater. 300 (2006) 192.
[19] R. Berger, J. Kliava, J.-C. Bissey, J. Appl. Phys. 87 (2000) 7389.
[20] R. Berger, J.-C. Bissey, J. Kliava, H. Daubric, C. Estournes, J. Magn. Magn. Mater. 234 (2001) 535.
[21] N. Krivoruchko, A.I. Marchenko, A.A. Prokhorov, Low Temp. Phys. 33 (2007) 433.
[22] G. Abramova, A. Pankrats, G. Petrakovskii, J.C.E. Rasch, M. Boehm, A. Vorotynov, V. Tugarinov, R. Szumszak, A. Bovina, V. Vasil'ev, J. Appl. Phys. 107 (2010) 093914.
[23] A.I. Pankrats, A.M. Vorotynov, V.I. Tugarinov, S.M. Zharkov, D.A. Velikanov, G. M. Abramova, G.M. Zeer, K. Ramasamy, A. Gupta, J. Appl. Phys. 116 (2014) 054302.
[24] K. Ramasamy, H. Sims, R.K. Gupta, D. Kumar, W.H. Butler, A. Gupta, Chem. Mater. 25 (2013) 4003.
[25] K. Ramasamy, H. Sims, S. Keshavarz, N. Naghibolashrafi, A. Gupta, J. Mater. Chem. C 4 (2016) 3628.
[26] V.I. Tugarinov, I.Ya. Makievskii, A.I. Pankrats, Instrum. Exp. Tech. 47 (2004) 472.
[27] I. Nakatani, H. Nose, K. Masumoto, J. Phys. Chem. Solids 39 (1978) 743.
[28] C. Bean, J.D. Livingston, J. Appl. Phys. 30 (1959) 120S.
[29] W.C. Nunes, L.M. Socolovsky, J.C. Denardin, F. Cebollada, A.L. Brandl, M. Knobel, Phys. Rev. B 72 (2005) 212413.
[30] W. Wernsdorfer, E.B. Orozco, K. Hasselbach, A. Benoit, B. Barbara, N. Demoncy, A. Loiseau, H. Pascard, D. Mailly, Phys. Rev. Lett. 78 (1997) 1791.
[31] A.D. Balaev, S.V. Semenov, A.A. Dubrovskiy, S.S. Yakushkin, V.L. Kirillov, O.N. Martyanov, J. Magn. Magn. Mater. 440 (2017) 199.